Cambridge Centre for Computational Chemical Engineering

University of Cambridge

Department of Chemical Engineering

Preprint ISSN 1473 – 4273

Detailed Modelling of Soot Formation in a Partially Stirred Plug Flow Reactor

M. Balthasar, F. Mauss [1], A. Knobel, M. Kraft [2]

submitted: 16th January 2003

[1] Division of Combustion Physics
Lund Institute of Technology
Box 118, S-221 00 Lund
Sweden

[2] Department of Chemical Engineering
University of Cambridge
Pembroke Street
Cambridge CB2 3RA
UK
E-Mail: markus_kraft@cheng.cam.ac.uk

Preprint No. 1

c4e

Key words and phrases. Carbon Black formation, Stochastic Reactor Model, PDF Transport equation .

Edited by
Cambridge Centre for Computational Chemical Engineering
Department of Chemical Engineering
University of Cambridge
Cambridge CB2 3RA
United Kingdom.

Fax: + 44 (0)1223 334796
E-Mail: c4e@cheng.cam.ac.uk
World Wide Web: http://www.cheng.cam.ac.uk/c4e/

Abstract

The purpose of this work is to propose a detailed model for the formation of soot in turbulent reacting flow and to use this model to study a carbon black furnace. The model is based on a combination of a detailed reaction mechanism to calculate the gas phase chemistry, a detailed kinetic soot model based on the method of moments, and the joint composition probability density function (PDF) of these scalar quantities.

Two problems, which arise when modelling the formation of soot in turbulent flows using a PDF approach, are studied. A consistency study of the combined scalar-soot moment approach reveals that the molecular diffusion term in the PDF-equation can be closed by the IEM and Curl-type mixing models. An investigation of different kernels for the collision frequency of soot particles shows that the influence of turbulence on particle coagulation is negligible for typical flame conditions and the particle size range considered.

The model is used as a simple tool to simulate a furnace black process, which is the most important industrial process for the production of carbon blacks. Despite the simplifications in the modelling of the turbulent flow reasonable agreement between the calculated soot yield and data measured in an industrial furnace black reactor is achieved although no adjustments were made to the kinetic parameters of the soot model. The effect of the mixing intensity on soot yield and different soot formation rates is investigated. In addition the influence of different operating conditions such as temperature and equivalence ratio in the primary zone of the reactor is studied.

Contents

1 INTRODUCTION **1**

2 MODELLING **3**

2.1 Soot Model 3

2.2 PDF Method 5

2.3 The PaSPFR Model 7

2.4 Investigation of the particle collision frequency in turbulent flows . . . 8

2.5 Investigation of consistency between MDF-PSDF and MDF-Moment formulation 9

3 SIMULATION OF A CARBON BLACK REACTOR **10**

3.1 Model Setup 10

3.2 Test Simulation 12

3.3 Comparison of the IEM and Curl models 13

3.4 Effect of Turbulent Mixing Time on Particle Properties 13

3.5 Effect of the Air to Fuel Ratio in the Primary Reactor 17

4 CONCLUSIONS **18**

5 ACKNOWLEDGEMENTS **19**

A Appendices **23**

A.1 Consistency of IEM mixing model 23

A.2 Consistency of Curl's Mixing Model 23

A.3 Consistency of the Binomial Langevin model 24

1 INTRODUCTION

The formation of soot is of interest from two points of view: On the one hand, it is a major pollutant, formed during many combustion processes, such as those occurring within a Diesel engine. On the other hand, it is an important industrial product, mainly used for improving the structure of materials, (e.g. as a reinforcement filler in tire treads), but also as a black pigment due to its good pigmentation properties. Worldwide, carbon black is produced on a large scale (4748 Megatons, 1983) mainly via the furnace black process [38], [6], [40]. In this process as it is shown in **Figure 1**, fuel (oil or natural gas) is burnt under fuel lean conditions in the primary stage. In a secondary stage a feedstock, usually oil, is injected through an atomizer into the hot exhaust from the primary stage. After the reaction mixture is quenched with water and cooled in heat exchangers, the carbon black is collected from the tail gas using a filter system. Depending on the operating conditions different grades of carbon black with differing properties (e.g. size and surface area) are produced. Specific applications require a certain grade of carbon black. It is therefore of importance to understand the impact of furnace settings on the grade of the produced carbon particles. In order to improve product quality and yield, reactor geometry and other process parameters have to be optimised. This is usually done through a large set of costly trial experiments. A precise physical understanding of the soot formation process and its interaction with the turbulent fluid flow is necessary to find the sensitivity of the various parameters, which can in turn lead to a shortening of the design cycle. This, and the fact that it is possible to study furnace conditions where experimental data are either not available or experiments cannot be performed, motivate the use of reliable models. For the purpose of simulating

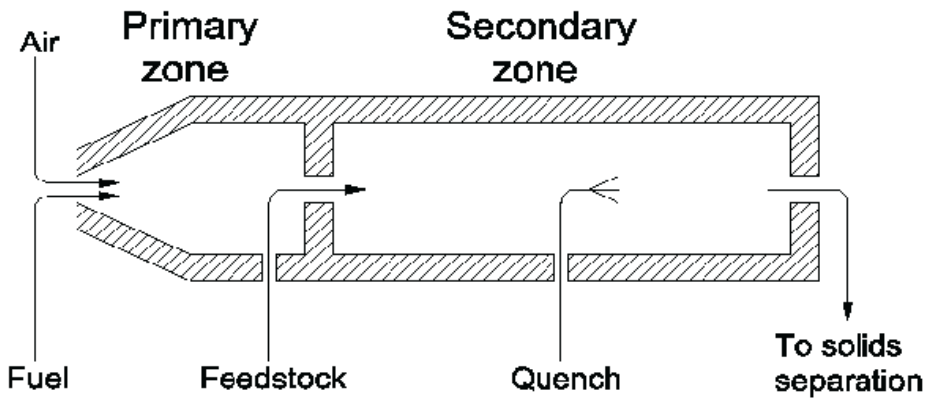

Figure 1: *Schematic diagram of a carbon black furnace. Gaseous fuel and air are burned under lean conditions in the first stage of the reactor. Oil is injected into the hot exhaust stream at the entrance of stage 2. The residence time in the second stage is controlled by a movable device quenching the flame by water droplet injection.*

soot production under turbulent conditions it is necessary to combine the modelling of the turbulent fluid flow with a model describing the formation of soot, the two processes being strongly coupled. Numerous approaches for the modelling of soot exist, many of which are discussed in the review article by Kennedy [19]. These approaches can be classed into three categories, namely, empirical models, models based on first principles, and a combination of the two. Empirical soot models make use of experimental data to predict quantities of interest; however, these models are only useful if the simulation conditions are close to the gauge experiments on which the models are based. The second class of soot models is based on a detailed description of the chemical and physical processes of soot formation. Although first principle models might not predict soot formation in a particular combustor as well as an empirical model, they are valid over a far larger range of conditions.

In this work we use a detailed model based on the work of Frenklach and Wang (e.g. [11], [18], [12]) to describe the kinetics of soot formation. As described below, the model centres on keeping track of the moments of the soot particle size distribution function (PSDF). This model in turn needs to be coupled to an approach describing turbulent reactive flows. The nature of turbulent flow lends itself to a statistical description. In this approach the physical quantities are assumed to be random variables, the spatial and temporal changes of these are then determined by a transport equation of their probability density function (PDF). Alternatively, transport equations for the statistical moments of the PDF, such as the mean and variance, can be used. In both cases the transport equations contain unclosed terms. In the case of the moment formulation the mean reaction rate is closed while the term describing molecular mixing needs to be supplied in the PDF approach. Solutions to these closure problems exist for fast chemistry. For example, the flamelet model, which is based on a fast chemistry assumption, has been successfully applied in combination with a detailed soot model (e.g. [29],[1]). However, in the distributed combustion regime the flamelet approach has limited value.

Various methodologies for combined soot and turbulence modelling can be found in the literature. Apart from empirical soot models for turbulent reactors, e.g. [3],[15], semi-empirical models based on the moment approach (e.g. [9],[36]) and on the PDF transport equation (e.g. [20],[13]) have been used to simulate laboratory flames and practical combustion devices. Yoshihara et al. [41] combined a detailed soot model with a stochastic mixing model for the prediction of soot emissions in a Diesel engine

The purpose of this paper is to present a modelling approach describing soot formation in turbulent reacting flows based on a PDF transport equation in general, and to simulate the formation of carbon black in a well-stirred reactor using this approach with a simplified adaptation of the PDF model, i.e. the partially stirred plug flow reactor PaSPFR model.

This paper can be divided into two parts. In the first part we describe how a soot model based on the moments of the PSDF can be combined with a probability density function (PDF) description of the turbulent flow. Brief summaries of the soot, the PDF and the PaSPFR models are given. Two issues which arise, the effect

of turbulence on the frequency of soot particle collision, and the consistency of the PSDF moments approach with various PDF based mixing models, are discussed.

In the second part, the model is used to simulate the industrial production of carbon black by the furnace black process, and to study the effect of mixing intensities and various operating parameters on the properties of carbon black.

2 MODELLING

This section summarizes the key elements of the probability density function based soot model. Firstly the soot and chemistry model is described, and the effect of turbulence on the particle collision frequency kernel is investigated. It is then demonstrated how the detailed soot model can be incorporated into the PDF transport equation. Following this, the partially stirred plug flow reactor model, derived from the full PDF transport equation, is briefly described. Finally the suitability of various PDF mixing models when applied to soot PSDF moments is investigated.

2.1 Soot Model

The soot model described here has been developed to model the formation of soot in laminar premixed and non-premixed flames. The basic physical and chemical processes assumed to be important for the formation of soot are: particle inception, coagulation, condensation and heterogeneous surface reactions, i.e. surface growth and oxidation by OH and O_2. The dynamics of the soot particle characteristics can be described by a set of equations for the moments of the soot particle size distribution function [12]:

$$\frac{dM_r}{dt} = \dot{M}_{r,pi} + \dot{M}_{r,con} + \dot{M}_{r,coag} + \dot{M}_{r,sr}, \tag{1}$$

where $\dot{M}_{r,pi}$, $\dot{M}_{r,con}$, $\dot{M}_{r,coag}$, $\dot{M}_{r,sr}$ are the rates of particle inception, condensation, coagulation and heterogeneous surface reactions for the r-th moment of the PSDF respectively. The moments are defined as:

$$M_r = \sum_{i=1}^{\infty} i^r N_i \,, \tag{2}$$

where N_i is the number density of soot particles of size class i. The zero-th moment is related to the mean number density, whereas the first moment is related to the mean mass or mean volume of the soot particles. Equations for the first four moments are solved in this study.

The coagulation rate of soot particles is determined from Smoluchowski's equation [39]:

$$\dot{M}_{0,coag} = \frac{1}{2} \sum_{i=1}^{\infty} \sum_{j=1}^{\infty} \beta_{i,j} N_i N_j, \tag{3}$$

$$\dot{M}_{r,coag} = \sum_{k=1}^{r-1} \binom{r}{k} \sum_{i=1}^{\infty} \sum_{j=1}^{\infty} i^k j^{r-k} \beta_{i,j} N_i N_j, \quad r = 2, 3, \ldots . \tag{4}$$

Coagulation does not contribute to the rate of M_1. It is assumed that the soot particles are spheres and that the spherical form is conserved during coagulation, i.e. the formation of aggregates is not taken into account. Under laminar conditions the frequency of particle collision, $\beta_{i,j}$, is due to Brownian motion and is dependent on the Knudsen number $Kn{=}\lambda/2d$, where λ is the gas mean free path and d the particle diameter. Following the approach of Kazakov and Frenklach [17], the coagulation rates used in this study are valid over the entire range of Knudsen numbers. The collision frequency, however, can increase in turbulent flows due to velocity fluctuations and inertial effects. The importance of this effect on the coagulation of soot particles as compared to Brownian coagulation is studied below.

Particle inception is modelled as the coagulation of two PAH molecules, where the PAH chemistry is described by a fast polymerisation approach using a steady-state assumption [25]. The rate of particle inception is described by a modified Smoluchowski equation:

$$\dot{M}_{r,pi} = \sum_{k=0}^{r} \binom{r}{k} \sum_{i=1}^{\infty} \sum_{j=1}^{\infty} i^k j^{r-k} \beta_{i,j} N_i^{PAH} N_j^{PAH}, \tag{5}$$

where N_i^{PAH} andN_j^{PAH} are the number densities of PAH-molecules of size class i and j. In evaluating the collision frequency, it is assumed that the two colliding PAH molecules are of similar size.

Condensation, i.e. the deposition of PAH molecules on the soot surface, is modelled as the coagulation of soot particles and PAH-molecules:

$$\dot{M}_{r,\,con} = \sum_{k=0}^{r-1} \binom{r}{k} \sum_{i=1}^{\infty} \sum_{j=1}^{\infty} i^k j^{r-k} \beta_{i,j} N_i N_j^{PAH} \ , \ r \neq 0. \tag{6}$$

Particle number density, i.e. M_0, is not changed due to condensation. The collision frequency of soot particles and PAH molecules is calculated by assuming that soot particles are much larger than the PAH molecules ($i >> j$).

Heterogeneous surface growth is accomplished by a repeating cycle of H-radical abstraction and acetylene addition, followed by the formation of a new aromatic ring on the soot surface (HACA-mechanism) [12]. Soot particle oxidation by molecular oxygen and OH-radicals is taken into account. The rates of heterogeneous surface reactions can be described by the following equation:

$$\dot{M}_{r,sr} = k_s C_g \alpha \chi_s \sum_{i-1}^{\infty} \sum_{k=0}^{r-1} \binom{r}{k} m_i^k \Delta^{r-k} S_i N_i, \tag{7}$$

where k_s is the rate coefficient, C_g the concentration of the gaseous species involved in the reaction, α the fraction of active surface sites, χ_s the number density of surface

sites and Δ the mass change; m_i, S_i and N_i are the mass, surface area, and number density of the i-th particle respectively.

A reaction mechanism containing 83 chemical species and 450 gas phase reactions is used to model fuel oxidation and pre-particle chemistry [12], [25], [4]. This mechanism has been applied in combination with the above mentioned soot model in several studies of soot formation in laminar flames under premixed and non-premixed conditions and has been shown to agree well with experimental data [25] [27] [26] [28]. The model constants for the gas phase mechanism and the soot model obtained from laminar flames have not been modified for use in this study. Radiation from gas phase species and soot particles has been taken into account in the optically thin limit.

2.2 PDF Method

In principle, soot formation in turbulent combustion can be described by the transport equations for the individual chemical species, the soot particle size moments and the energy conservation equation, along with the Navier Stokes and continuity equations. However, this equation system cannot be solved numerically due to the high computational cost and difficulty in defining suitable boundary conditions. One alternative to a direct numerical simulation is the use of statistical methods. The unknown quantities such as velocities, temperature or composition are viewed as random variables. Time and spatial evolution of these random variables are then given by a transport equation for their joint PDF. A detailed description of this approach is given by Pope [31]. Here we combine the detailed soot model based on the moments of the soot particle size density function, with the joint scalar PDF transport equation; however, in principle this model can also be included in a more complete description of turbulent reactive flow as given by the joint velocity-frequency-composition PDF transport equation [32]. The unknown scalar quantities to be calculated are 83 chemical species mass fractions, enthalpy and the first four moments of the soot particle size distribution. These can be written as the joint scalar random vector

$$\underline{\phi} = (Y_1, ..., Y_{83}, h, M_0, M_1, M_2, M_3)^T. \tag{8}$$

At a given location $\underline{x}$ and time t, this vector has a corresponding joint scalar PDF, $f_{\underline{\phi}}(\underline{\psi}, \underline{x}, t)$. Following Pope [31], for inhomogeneous variable-density flows we use the joint scalar mass density function (MDF), defined as

$$F_{\underline{\phi}}(\underline{\psi}, \underline{x}, t) = \rho(\underline{\psi}) f(Y_1, ..., Y_{83}, h, M_0, M_1 M_2, M_3, \underline{x}, t). \tag{9}$$

The temporal and spatial evolution of the MDF is given by the following transport equation.

$$\begin{aligned} &\frac{\partial}{\partial t} F_{\underline{\phi}}(\underline{\psi}, \underline{x}, t) + \frac{\partial (\tilde{U}_i F_{\underline{\phi}}(\underline{\psi}, \underline{x}, t))}{\partial x_i} + \frac{\partial}{\partial \psi_k} \left(S_k(\underline{\psi}) F_{\underline{\phi}}(\underline{\psi}, \underline{x}, t) \right) \\ &\qquad = \frac{\partial}{\partial \psi_k} \left(\left\langle \frac{1}{\rho} \frac{\partial J_i^k}{\partial x_i} \middle| \underline{\psi} \right\rangle F_{\underline{\phi}}(\underline{\psi}, \underline{x}, t) \right) - \frac{\partial}{\partial x_i} (\left\langle u_i'' \middle| \underline{\psi} \right\rangle F_{\underline{\phi}}(\underline{\psi}, \underline{x}, t)) \end{aligned} \tag{10}$$

Where $\tilde{U}_i$ is the mean velocity of the turbulent flow, S_k the chemical production rate of species k, ρ the density, J_i^k the diffusive flux vector and $u_i^{''}$ the turbulent velocity fluctuations.

The second term on the right hand side of Eq.(10) describes the transport of the PDF in physical space due to velocity fluctuations. This term is usually modelled by the gradient diffusion assumption

$$\left\langle u_i^{''} \,|\underline{\psi}\right\rangle F_{\underline{\phi}}(\underline{\psi},t) = -\Gamma_T \frac{1}{\langle\rho\rangle}\frac{\partial F_{\underline{\phi}}}{\partial x_i}. \tag{11}$$

The first term on the right hand side of Eq.(10) describes the time evolution of the PDF in scalar space due to turbulent diffusion and requires further modelling. Many different models of varying degrees of complexity and physical relevance [31] have been developed to close this term. In this paper we focus on three mixing models taken from the literature that have been used for the simulation of turbulent flames. In order to demonstrate the problem arising when the moments of the soot PSDF are mixed, we state the mixing models in terms of an evolution equation for stochastic particles. Stochastic particles are required when solving Eq.(10) by means of a Monte Carlo algorithm, in which an ensemble of Nstochastic particles is used to approximate the MDF.

The simplest model for turbulent diffusion is the interaction by exchange with the mean (IEM) model (also known as the linear mean square estimator (LMSE) model) [7]. The evolution due to turbulent diffusion for the n-th stochastic particle is given by an initial position in scalar space and the following equation

$$\frac{d}{dt}\underline{\psi}^{(n)} = -\frac{1}{2}\frac{C_\phi}{\tau}(\underline{\psi}^{(n)} - \langle\underline{\phi}\rangle). \tag{12}$$

This model implies that the property of a stochastic particle moves towards the average of that property taken over all stochastic particles.

The constant, C_ϕ, is a model parameter and is chosen to give the correct decay rate of the variance. The turbulent time scale τ is a measure of the intensity of the turbulence in the flow, and has to be supplied. This can be done by coupling the MDF transport equation with a standard finite volume CFD code.

The second mixing model is a so-called particle interaction model. Here pairs of stochastic particles are chosen (according to a certain probability law characteristic of the particular model) and mixed to produce two new stochastic particles. The simplest particle interaction method is Curl's model [5]. One pair at a time is selected and the properties of the two post-mixed stochastic particles are the mean of the properties of the original particles. A disadvantage of this method is that the transition probability is not continuous. In a modification of Curl's model, developed independently by Janicka et al. [16] and Dopazo [8], the extent of the mixing is determined by a uniformly distributed random variable α. The mixing rules for a pair of stochastic particles are then given by:

$$\begin{aligned}\underline{\psi}^{(n)}(t+\Delta t) &= (1-\alpha)\underline{\psi}^{(n)}(t) + \tfrac{1}{2}\alpha(\underline{\psi}^{(n)}(t) + \underline{\psi}^{(m)}(t)),\\ \underline{\psi}^{(m)}(t+\Delta t) &= (1-\alpha)\underline{\psi}^{(m)}(t) + \tfrac{1}{2}\alpha(\underline{\psi}^{(n)}(t) + \underline{\psi}^{(m)}(t)),\end{aligned} \tag{13}$$

$$0 \leq \alpha \leq 1 \quad .$$

This method produces a continuous PDF; however, the final shape is not Gaussian as desired [30]. Specifically the forth and higher even standardised moments are infinite for the final distribution, whereas a Gaussian distribution retains finite standardised moments. To address these problems, further modifications to Curl's model have been made, but are not considered here [30].

The third model we consider is the Binominal Langevin model, developed by Valiño and Dopazo [37]. In this model a property of a stochastic particle moves towards the average of all stochastic particles (similar to, but formulated differently to the IEM model). However, superimposed on this drift towards the mean is a random noise or fluctuation that blurs the PDF. The full expression for a stochastic particle is:

$$\begin{aligned} d\underline{\psi}^{(n)}(t) = &-\frac{C_\phi}{2\tau}\left(1 + k_{BL}(1 - \frac{\langle \underline{\phi'^2} \rangle}{\psi_*^2}\right)(\underline{\psi}^{(n)} - \langle \underline{\phi} \rangle)dt \\ &+ \left(k_{BL}\frac{C_\phi}{2\tau}\left(1 - \frac{(\underline{\psi}^{(n)} - \langle \underline{\phi} \rangle)^2}{\psi_*^2}\right)\langle \underline{\phi'^2} \rangle\right)^{\frac{1}{2}} dW_{bl}, \end{aligned} \tag{14}$$

where dW_{bl} is the increment of a binomial stochastic process. In this method the PDF relaxes asymptotically to a Gaussian and results display excellent agreement with previous direct numerical simulations.

2.3 The PaSPFR Model

Although spatially resolved numerical simulations of the full joint composition MDF transport equation have already been performed [2], it is not feasible to use this method for the analysis of large chemical systems and parametric studies of operating conditions in industrial devices as the computational time and storage requirements are prohibitive. Therefore, at present, it is necessary to introduce some simplifying assumptions. Analogously to the plug flow reactor (PFR) and the perfectly stirred reactor (PSR) models, both of which are based on assumptions of homogeneity, it is possible to derive partially stirred plug flow reactor (PaSPFR) and partially stirred reactor (PaSR) stochastic models based on the assumption of statistical homogeneity of the scalar variables. This means that we assume that the joint PDF does not vary in space. The derivation of these stochastic reactor models is described by Kraft [21]. In the case of the PaSPFR, the MDF is only a function of composition and distance along the reactor, which can in turn be transformed into a residence time. The transport equation for the MDF is then

$$\frac{\partial}{\partial t}F_{\underline{\phi}}(\underline{\psi}, t) + \frac{\partial}{\partial \psi_k}\left(S_k(\underline{\psi})F_{\underline{\phi}}(\underline{\psi}, t)\right) = \frac{\partial}{\partial \psi_k}\left(\left\langle \frac{1}{\rho}\frac{\partial J_i^k}{\partial x_i} \,\middle|\, \underline{\psi} \right\rangle F_{\underline{\phi}}(\underline{\psi}, t)\right). \tag{15}$$

This equation still contains the unclosed term for turbulent diffusion, which must be replaced by a suitable mixing model. Practical devices are then modelled by a combination of these simple stochastic reactor models. Although the assumption of spatial homogeneity is an oversimplification of reality, the PaSPFR has successfully

been used for the prediction of the products of incomplete combustion in a simple bench scale reactor [33],[22]. In this paper we employ the PaSPFR model with the detailed soot model to simulate the production of carbon black.

2.4 Investigation of the particle collision frequency in turbulent flows

The soot model described above was originally developed for laminar flames; consequently any potential enhancement of coagulation due to turbulence was tested by comparing the collision frequency of particles in turbulent flow to that due to Brownian coagulation [35].

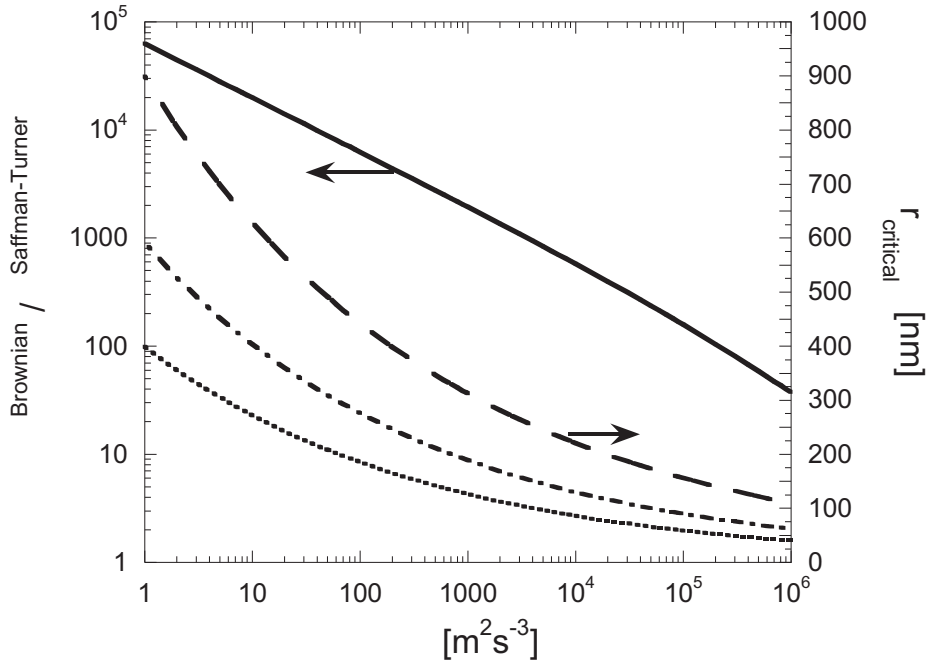

Figure 2: *Comparison of the Brownian and the Saffman-Turner collision frequency as a function of turbulent energy dissipation rate at $T = 1800K$, $r_a = r_b$=50nm and p=1bar (solid line). Also shown is the critical radius at which Brownian coagulation is equal to turbulent coagulation, at pressures of p=1bar (long-dashed line), p=10bar (dashed-dotted line), p=100bar (dotted line).*

The analysis of Saffman and Turner [34] gives the collision frequency for particles surrounded by a turbulent flow as:

$$\beta_{a,b}^{ST} = 2\sqrt{2\pi}(r_a + r_b)^2 \left[1.3(\tau_a + \tau_b)^2 \varepsilon^{3/2} \nu^{-1/2} + (r_a + r_b)^2 \varepsilon \nu^{-1}/9\right]^{1/2}, \qquad (16)$$

where r_a and r_b are the radii of particle a and b, ν is the kinematic viscosity, which was taken to be that of nitrogen, and ε is the turbulent energy dissipation rate. τ_a

and τ_b are defined as $\tau_x = (2r_x^2\rho_S)/(9\mu)$ where μ is the dynamic viscosity. In Eq.(16) gravitational forces have been neglected. The ratio of the Brownian to the Saffman-Turner collision frequency at a temperature of T =1800K for equal sized particles with $r_a = r_b$ =50nm is shown in **Figure 2**. Brownian coagulation is the dominant process even at very high rates of turbulent energy dissipation. In addition, **Figure 2** displays the critical radius (defined as the particle radius ($r_a = r_b$) at which both coagulation frequencies are equal) for three different pressures (p=1, 10, 100 bar). The critical radius at a pressure of 1 bar never exceeds the radius of soot particles normally found in flames of that pressure [14]. At larger pressures the critical radius decreases and is shifted towards lower dissipation rates. For very high-pressures (e.g. those found in Diesel engines) and large particle sizes, turbulence could in fact increase soot particle coagulation. Since the furnace black process, studied below, is operated at 1 bar, turbulent coagulation can be neglected.

2.5 Investigation of consistency between MDF-PSDF and MDF-Moment formulation

The MDF of the chemical species and the moments of the PSDF at a location $\underline{x}$, is given by

$$F^{(1)}(Y_1, ..., Y_{83}, h, M_0, M_1, M_2, M_3, \underline{x}, t). \tag{17}$$

Alternatively, one can consider a MDF based on the chemical species and the PSDF directly

$$F^{(2)}(Y_1, ..., Y_{83}, h, N_1, N_2, N_3, ..., \underline{x}, t). \tag{18}$$

The evolution of both MDFs is described by the transport equation (Eq.(10)). It is a necessary requirement that the solution $F^{(1)}$ can be derived from the solution $F^{(2)}$, i.e. formulation one must be consistent with formulation two. If the two formulations are consistent at the beginning and each operator in Eq.(10) is consistent then the two formulations are consistent. Since the operators that transport N_i in physical space (i.e. convection and gradient diffusion) are independent of N_i, consistency is clear. However, the operators that transport N_i in scalar space are dependent onN_i. These operators describe the chemical reactions and turbulent mixing. The term that describes chemical reaction is consistent by definition; therefore the only term that needs to be examined is that which describes turbulent diffusion. Consistency on the level of stochastic particles means that the dynamics of the moments of the PSDF calculated from $N_i^{(n)}(t)$must be the same as the dynamics of $M_r^{(n)}(t)$. This must also apply to any function of these quantities. **Figure 3** illustrates the conditions for consistency in the case of the statistical moments. Depending on the choice of formulation, there are two methods of calculating the dynamics of the statistical moments. The first method is to apply the mixing model to $N_i^{(n)}(t)$ and then calculate the moments from all stochastic particles. Alternatively, one can calculate the moments of the PSDF and then apply the mixing model. Crucially both methods have to give the same answer at each point in time. If this is not

the case then the mixing model used is inconsistent with the method of PSDF-moments. Appendix (A1-A3) contains the consistency checks for the three mixing models (IEM, Curl-type and binomial Langevin). It is shown that the IEM and Curl models are consistent. Consequently, the IEM and Curl models are used in the simulation of the carbon black furnace process.

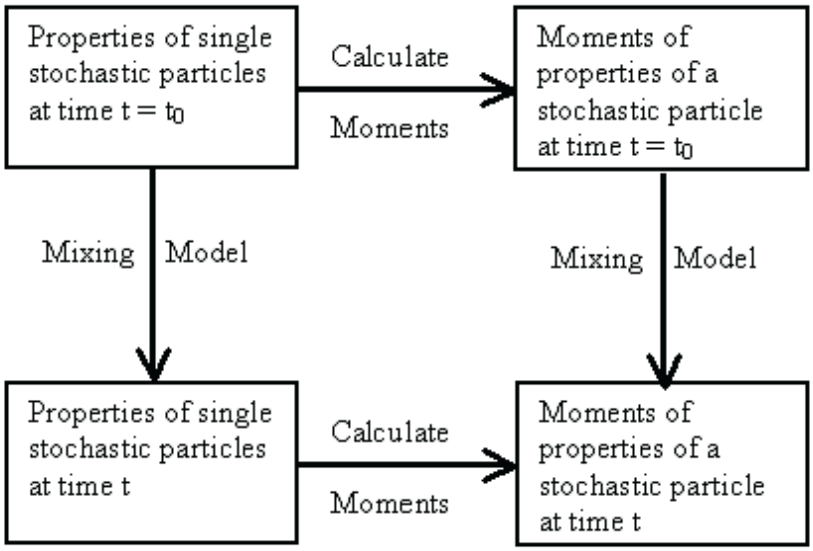

Figure 3: *Illustration of mixing model consistency procedure.*

3 SIMULATION OF A CARBON BLACK REACTOR

To demonstrate the above soot/PaSPFR model, a simulation of an industrial carbon black reactor was developed.

3.1 Model Setup

In this simulation the primary stage is modelled as a perfectly stirred reactor (PSR), while the second stage uses the PaSPFR model. This is illustrated in the model flow sheet in **Figure 4**, in which various model parameters are also shown. Apart from the simplifications inherent in the PaSPFR model as discussed above, two further simplifying assumptions are made. Firstly, it is assumed that the turbulent time scale (τ) is constant along the length of the reactor, i.e. τ=*1.339 ms*. This turbulent time scale was obtained from CFD calculations performed by Lockwood et. al. [24]

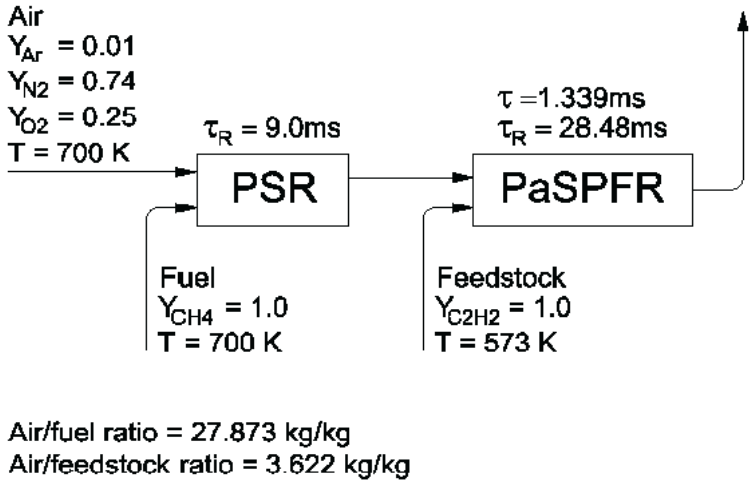

Figure 4: *Process flow diagram of the carbon black furnace simulation. The shown conditions are identical to those used by Lockwood and van Niekerk [24], which used experimental data from [10] in combination with additional parameters from [6], representing conditions for the production of a N330 grade carbon black.*

where it is given at one point in the flow field only. The model is however capable of using a variable mixing time over reactor length, which would be a more realistic description of the mixing process.

Secondly, although in reality an aromatic oil is the usual feedstock, here we use acetylene. The primary reason for the second assumption is that the kinetic mechanism used has been well validated for acetylene but not for aromatics. In addition the carbon to hydrogen ratio of acetylene is close to that of aromatic hydrocarbons. In any event, reactor operating conditions rather than feedstock composition have the greater effect on carbon black properties [38].

In the simulations below, the mean values of the following variables are predicted: Carbon mass fraction (Y_S), yield (kg of carbon per kg of feedstock), particle number density (N), soot volume fraction (f_v), soot particle diameter (d_p) and specific surface area (A).

As discussed above the particle number density and soot volume fraction can be determined from the zero-th and first moments of the soot PSDF. Assuming that the particles remain spherical, the mean particle diameter can be calculated from:

$$d_p = \left(\frac{6m_1}{\pi \rho_s N_A} \frac{M_1}{M_0} \right)^{1/3}. \tag{19}$$

where m_1 is the molecular mass of the base unit from which the soot particles are constructed and N_A is the Avogadro number. The specific surface area is calculated

from:

$$A = \frac{6}{\rho_s d_p}. \tag{20}$$

3.2 Test Simulation

The first simulation tests the model against the simulation results and industrial data reported by Lockwood and van Niekerk [24]. In Ref. [24] the operation conditions for an industrial carbon black reactor and the corresponding experimental data from [10] were used in combination with additional parameters from [6]. The conditions in the present study are the same as used in [24] representing conditions for the production of a N330 grade carbon black. In particular, the same air to fuel (AFR), air to feedstock ratio (AOR), residence time (τ_R) and the turbulent time scale are used. (Note that the value of τ*=1.339 ms* is obtained from CFD-calculations in [24] is given at two diameters down the length of the reactor, but here is assumed to apply to the entire secondary zone). **Figure 4** summarizes the operating conditions of the base case simulation. Only overall exhaust values of the soot particle properties such as soot mass fraction, yield and size of the primary particles were available, which did not allow for a thorough verification of the model's predictive capability.

Table 1: *Base case simulation results compared to measured values in a carbon black furnace (actual).*

Variable	**Predicted (IEM)**	**Predicted (modified Curl)**	**Actual**
Exit gas temperature (K)	**1898**	**1906**	
Exit gas soot mass fraction (kg/kg)	**0.084**	**0.086**	**0.127**
Particle number density (m^{-3})	**6.00×10^{15}**	**5.41×10^{15}**	
Soot volume fraction (m^3/m^3)	**7.62×10^{-6}**	**7.86×10^{-6}**	
Primary particle diameter (nm)	**-**	**-**	**30**
Soot particle diameter (nm)	**134.3**	**140.5**	**-**
Specific surface area (m^2/g)	**24.81**	**23.72**	
Yield (kg carbon/kg feedstock)	**0.398**	**0.407**	**0.605**

Only exit gas soot mass fraction, yield and primary particle size were available for model validation. The measured particle diameter corresponds to the mean diameter of primary particles that comprise the soot agglomerates. Since the formation of agglomerates was not taken into account in the soot model and the soot particles were assumed to be spherical the discrepancy of the two diameters is obvious.

The results of the test simulation calculated using both the weighted IEM and modified Curl models are presented in Table 1. Since the IEM model does not result in a change to the shape of the PDF, and the two inlet streams to the secondary zone

are fully mixed, only two stochastic particles are required to represent the resulting double delta PDF. In contrast, 300 particles are used in the Curl simulation to represent the bell shaped PDF.

The difference between the IEM and Curl simulations is small. In both cases, the soot mass fraction and yield are under predicted by about 33%. Predicted primary soot particle diameter is significantly larger; however, this is due to the omission of agglomeration effects in the soot model (i.e. above a certain primary particle size, it is no longer reasonable to assume that the collision of two soot particles results in larger spherical particle). However, given the number of assumptions made in the formulation of the model and the fact that no changes have been made to the soot model parameters as calibrated for a laminar flame, the model predictions are fair. In particular the use of chemical models for aromatic oils as feedstock should increase the model prediction of the final soot mass.

3.3 Comparison of the IEM and Curl models

As discussed above the Curl model and its variants have an advantage over the IEM in that they better approximate the actual scalar probability density function (i.e. relaxation of the PDF, and with some modifications relaxation to a continuous or even a near Gaussian PDF). A disadvantage of the Curl model is that it requires a large number of stochastic particles to approximate the PDF, while two particles are sufficient when using the IEM model for this particular case. During the solution of the model the reaction kinetics of each of these particles need to be integrated, significantly increasing the computational time. Results from simulations conducted using the IEM and modified Curl show little difference between the two models. For example, **Figure 5** shows the predicted particle number densities and soot volume fractions as a function of residence time calculated using the two models for the mixing time that was used to simulate the carbon black reactor. Similarly temperature and other model variables show little difference. The difference between the two models increases however with increasing mixing time, i.e. slower mixing. Therefore, both the modified Curl and the IEM model were used for the sensitivity analysis and owing to the significantly lower computational costs the IEM model was used for the remaining simulations, i.e. the parameter study (**Figure 8**).

3.4 Effect of Turbulent Mixing Time on Particle Properties

The effect of the turbulent mixing time on the temperature and the properties of carbon black was investigated. A wide range of mixing times from τ*=0 ms* (i.e. the PaSPFR model becomes a PFR model) to τ =40ms were considered (note that a larger value of τ corresponds to slower mixing). **Figure 6** shows the temporal evolution of temperature, number density and soot volume fraction in the secondary zone of the reactor for a number of different values of τ(i.e. τ*=0, 0.1, 1, 5, 10 ms*) obtained with modified Curl model. The feedstock is mixed into the hot exhaust

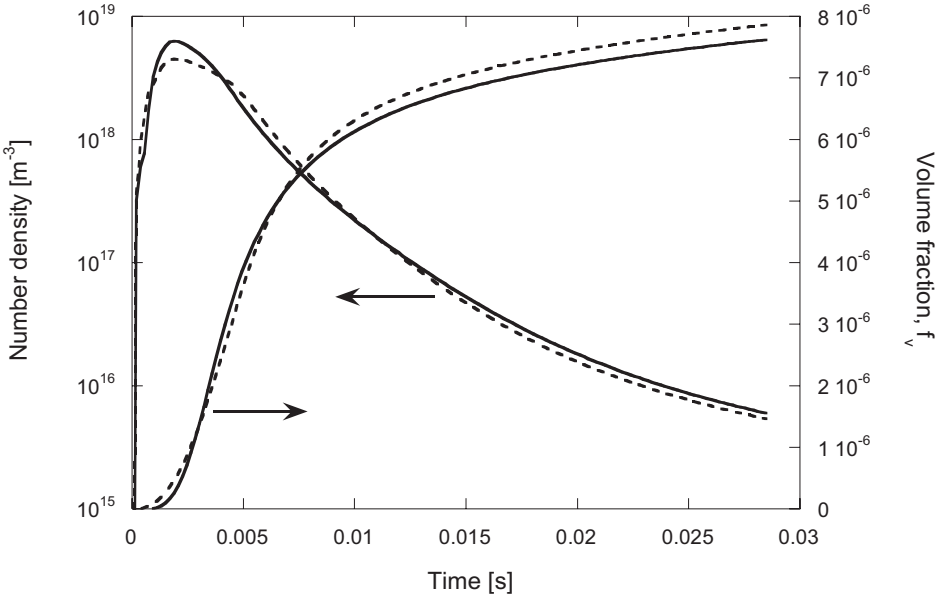

Figure 5: *Comparison of calculated particle number densities and soot volume fractions calculated using the IEM (lines) and the modified Curl (dashed lines) mixing models (Parameters as for the base case, τ=1.339 ms). The results obtained with both mixing models give nearly the same result for the shown scalars.*

gas from the first zone, which operates under lean conditions ($\Phi \approx 0.65$). Temperature increases slowly for the perfectly mixed case as the remaining oxygen from the first stage is consumed and reaches a maximum at $t \approx 9$ *ms*. For slower mixing (i.e. higher τ) the temperature shows a steeper increase in the first few milliseconds with the maximum temperature being slightly higher than for the perfectly mixed case. This is most pronounced for τ =1 *ms*. Going from τ=1 to *10 ms* the temperature profile changes significantly. The temperature gradient is much smaller but the final temperature is in the same range as for the other cases. Thus, the initial temperature profile for inhomogeneous mixtures as compared to a perfect mixture depends strongly on the mixing intensity. The initial slope of temperature is enhanced by fast mixing and reduced by slow mixing. In the transition from fast to slow mixing (τ=5 *ms*) the temperature profile exhibits a similar shape as for the perfectly mixed case. The overall equivalence ratio including the first and the second zone is clearly on the fuel rich side while conditions in the first zone are fuel lean. Thus, if a perfect mixing of the exhaust stream and the feedstock is assumed the mixture burns under fuel rich conditions. When taking inhomogeneities into account a certain amount of feedstock depending on the mixing intensity is mixed into the hot exhaust initially. If mixing is fast, the conditions in some of the stochastic particles are close to stoichiometric consequently leading to a steeper increase in temperature. This process is delayed for slower mixing and the temperature increases initially much slower than for the homogenous case.

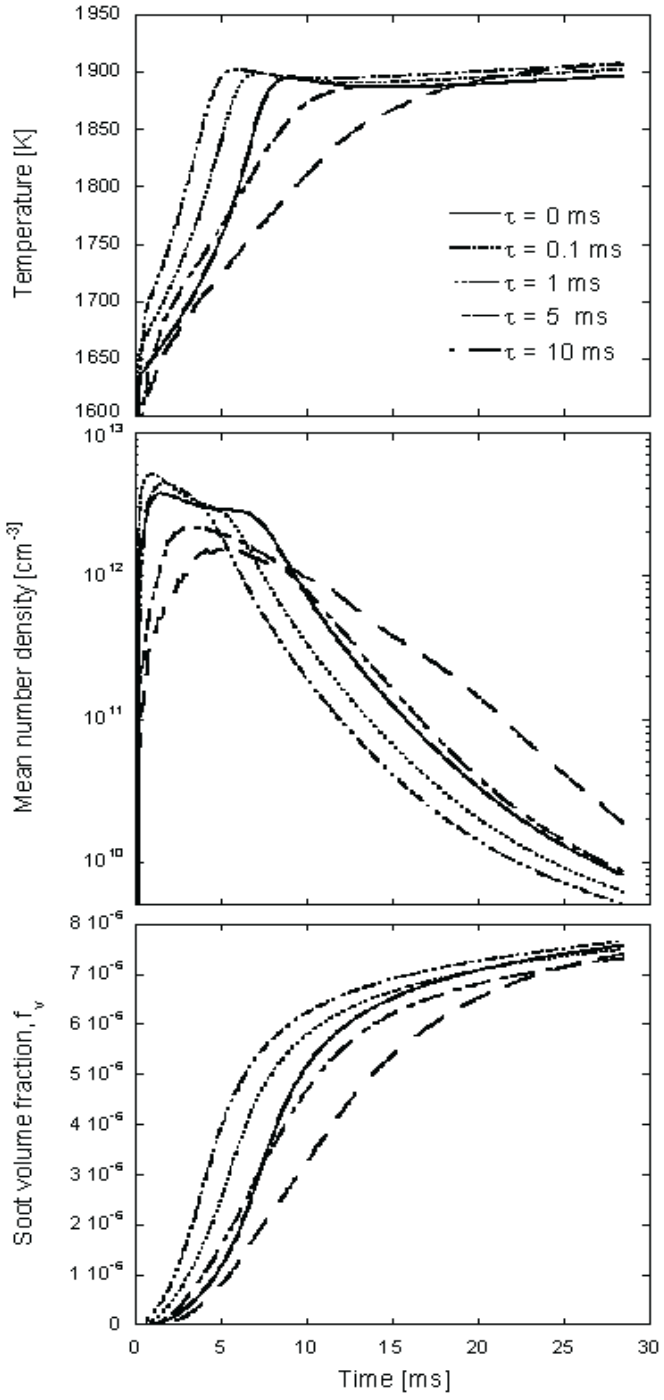

Figure 6: *Temperature, number density and soot volume fraction as a function of residence time in the secondary stage of the reactor where the feedstock is injected into the hot exhaust from the first stage. Results of a PFR calculation (full line), i.e. the feedstock and the hot exhaust are perfectly mixed, are compared to results assuming an inhomogeneous mixture at the entrance of the second stage. Results for different turbulent mixing times obtained with the modified Curl model are presented.*

Particles are formed during the first few milliseconds in the rich part of the mixture and decreases subsequently due to coagulation. The decrease in number density is more distinct for τ=*0.1* and *1 ms* since temperature is higher and thus coagulation rates faster. The peak in number density is decreasing for τ=*5* and *10 ms* but the number density at the exit is highest due to slower coagulation. The fact that final soot volume fractions are roughly identical for all cases but number densities are different indicates that the particles have different sizes at the exit of the reactor. Thus particle sizes are influenced by the intensity of mixing. The particles produced from the perfectly mixed case have a diameter of around *120 nm*. The size increases for τ=*0.1* and *1 ms* to a maximum value of around *140 nm* and decreases again to *91 nm* for the slowest mixing case. Note that the mixing time in the base case simulation (**Figure 5**), which was used to compare to experimental data, is τ=*1.339 ms*. The

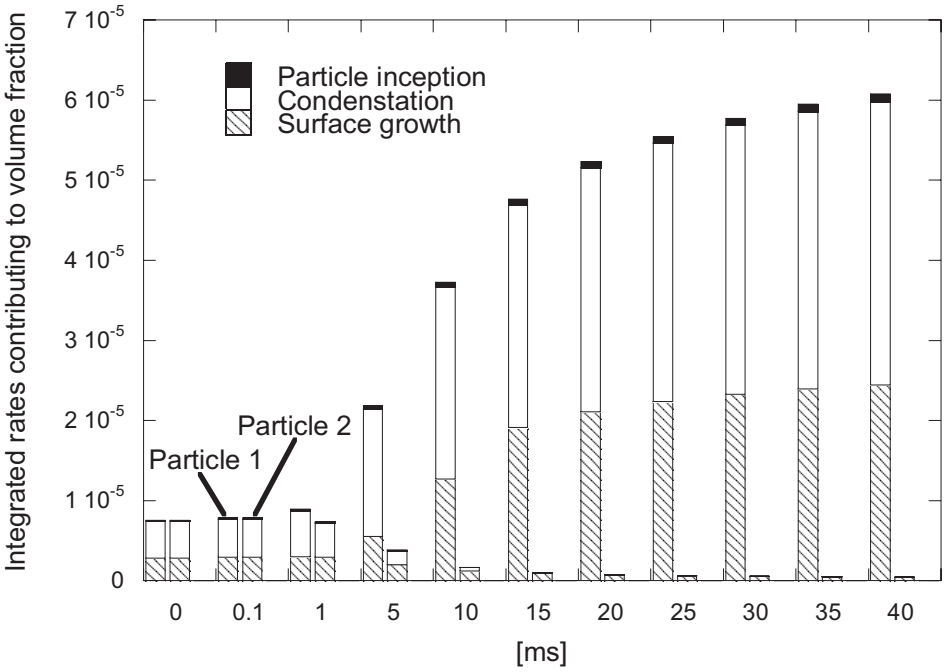

Figure 7: *Effect of mixing time on the integrated rates of processes contributing to soot volume fraction. At the inlet particle 1 represents the feedstock and particle 2 the hot burnt fuel/air mixture. At slower mixing times soot volume production in the feedstock particle dominates.*

effect of the various processes contributing to the increase in volume fraction can be investigated by integrating the rates of soot formation across the residence time of the reactor. Results from the IEM model are used in the following to illustrate the sensitivity of the rates of soot formation on the degree of mixing. **Figure 7** shows the integrated rates of particle inception, PAH condensation and surface growth for the two stochastic particles, at a number of different values of τ. Particle 1 represents initially the feedstock in which parts of the hot exhaust gas are being

mixed with increasing residence time. Particle 2 represents the hot burnt gas from the first stage of the reactor. In this particle 2 a portion of the feedstock is mixed and burnt with the exhaust from the first stage. At low (i.e. rapid) mixing times ($\tau < 5ms$) soot production is spread evenly between the two particles; however, as the mixing time is increased soot production in the feedstock particle dominates. It is remarkable that the condensation rate is slightly higher than the rate of surface growth by acetylene addition since in laminar premixed flames surface growth has been found to be the most important process for the mass growth of soot particles. The same kinetic parameters for surface growth as well as condensation as obtained in laminar premixed flames were however used in this study.

3.5 Effect of the Air to Fuel Ratio in the Primary Reactor

In the above studies a constant air to fuel ratio of *27.87 kg/kg* has been used. This corresponds to an equivalence ratio of Φ=*0.65* in the primary stage of the reactor. Being one of the most interesting parameters for practical applications the effect of varying the AFR was studied for values of Φ=*0.5* to Φ=*0.9* in the primary zone. Simultaneously, the turbulent mixing time was also varied between 0 and *15 ms*. Since one of the major aims of this study is the development of a simple tool to investigate sensitivities of particle formation in practical applications, the following results were obtained with the IEM model due to its apparent advantages in computational time. The results obtained from the IEM and modified Curl mode can however differ but emphasis was put on predicting tendencies rather than absolute values in this part of the study. **Figure 8** shows the particle number density and the soot yield at the exit of the reactor as a function of primary zone $\Phi$for different values of τ. The residence time in the second reactor was kept constant although in practice it would be decreased by higher equivalence ratios in the first reactor, due to the higher temperature and mass flux of the primary exhaust entering the second stage. Slower mixing (increasing τ) results in an increase in the particle number density at all values of primary Φ. This effect, however, is particularly pronounced at values of Φ close to unity, where the exit particle number density is two orders of magnitude higher. The number density increases while the yield decreases at high equivalence ratios and slow mixing since optimum conditions in terms of temperature and fuel/air equivalence ratio for the soot inception and growth are not reached until higher residence times. Hence at the reactor exit the soot formation process is not completed indicated by a high number density and a low soot yield. In contrast, at low values of Φslower mixing results in an increase in the yield; however, for equivalence ratios closer to unity the yield is high under conditions of fast mixing but drops off for slower mixing times.

For a constant τ of *1 ms* or less, the yield increases linearly with increasing primary Φ. The same trend was observed in Ref. [24]; however, for slow mixing the model predicts a reverse trend, i.e. the yield decreasing slightly for increasing equivalence ratio in the primary zone.

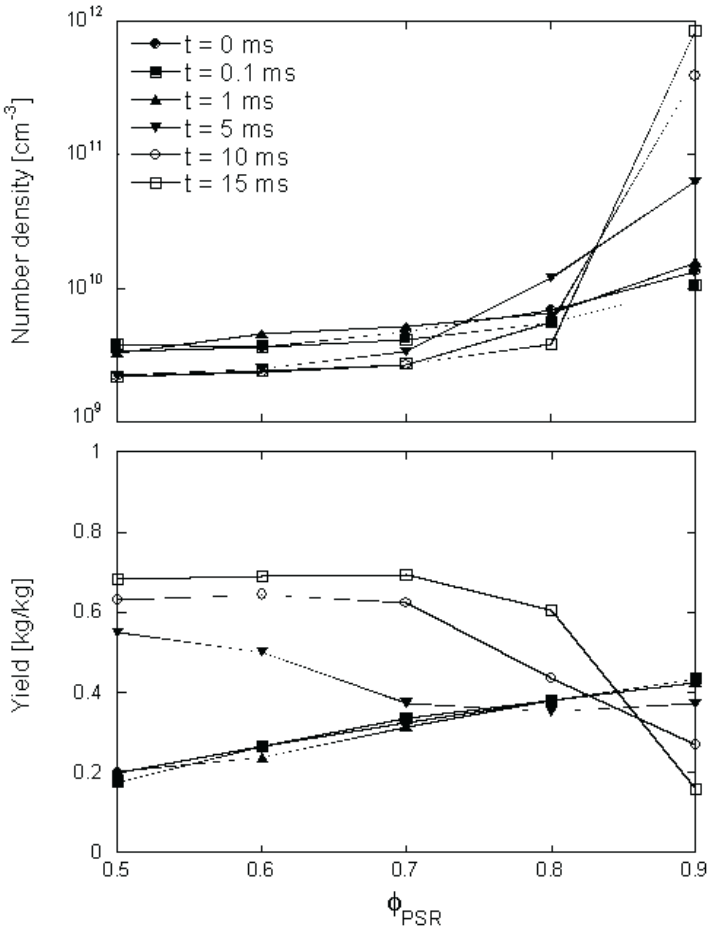

Figure 8: *Particle number density and overall yield (kg carbon/kg feedstock) in the exit stream as a function of mixing time and primary reactor equivalence ratio.*

4 CONCLUSIONS

An approach is presented that couples a detailed soot model based on the moments of the soot particle size distribution to a joint PDF transport equation describing turbulent reacting flows. Based on this approach we focus in this study on the simulation of soot formation in turbulent reacting flows in systems that can be described by a partially stirred plug flow reactor model. In particular the influence of turbulent mixing on chemical kinetics and the formation of soot is investigated in a reactor used for the production of carbon black.

The influence of turbulence on soot particle collision frequency is found to be of minor importance for the conditions of this study. The investigation of the consistency conditions of the combined scalar and soot moment approach shows that the IEM and the Curl models can be used to describe the mixing of the stochastic moments of the soot PSDF. A furnace black process is simulated and the results

compared to data of an industrial reactor. Simplifying assumptions on the turbulent flow in a particular reactor, leading to stochastic reactor models, have to be made to reduce computational cost. Results obtained using the IEM and the modified Curl model differ only slightly. The model predictions are in fair agreement to the measured data without making any adjustments to the soot model parameters have been made.

However, the model needs further extensions to be applicable as a predictive tool for the production of carbon black. To achieve a more realistic description of soot formation in a carbon black reactor, agglomeration of soot particles has to be taken into account. The evaporation of the feedstock could be included using a spray model. Future work also includes a better description of the turbulent flow and the intensity of mixing by using a time dependent mixing time, which could be obtained from CFD-simulations. Finally, the predictive capabilities of the model have to be validated over a wider range of operating conditions. In particular, it remains to be determined if changes in the soot particle properties caused by varying single operation parameters can be predicted accurately.

5 ACKNOWLEDGEMENTS

This work was supported by the Swedish Centre of Combustion Science and Technology, CECOST. One of the authors (mk) would like to acknowledge the support of A. Sarofim (University of Utah) within the framework of the CSAFE program.

References

[1] Bai, X. S., Balthasar, M., F., M. and Fuchs, L. (1998). *Proc. Combust. Inst.* **27**: 1623.

[2] Barlow, R., Bilger, R., Chen, J.-Y., Gokalp, I., Hassel, E., Masri, A. and Peters., N. (1996). *Proceedings of the International Workshop on Measurement and Computation of Turbulent Nonpremixed Flames*, See http://www.ca.sandia.gov/tdf/Workshop.html.

[3] Brown, A. J. and Heywood, J. B. (1988). *Combust. Sci. and Tech.* **58**: 195.

[4] Chevalier, C., Louessard, P., Mueller, U. C. and Warnatz, J. (1990). *Int. Symp. on Diagnostics and Modelling of Combustion in Internal Engines COMODIA 90, Kyoto.*

[5] Curl, R. (1963). *A.I.Ch.E.J.* **9**: 175.

[6] Dannenberg, E. (1978). *Encyclopedia of Chemical Technology (Vol. 4), 3rd Ed*, John Wiley and Sons, New York.

[7] Dopazo, C. (1975). *Phys. of Fluids* **18**: 397.

[8] Dopazo, C. (1979). *Phys. of Fluids* **22**: 20.

[9] Fairweather, M., Jones, W. P. and Lindstedt, R. P. (1992). *Combust. Flame* **89**: 45.

[10] Forseth, G. J. and Jones, W. R. (1983). *R & D Report*, Phillips Petroleum Company, pp. 9633–83.

[11] Frenklach, F. and Wang, H. (1990). *Proc. Combust. Inst.* **23**: 1559.

[12] Frenklach, M. and Wang, H. (1994). *Soot Formation in Combustion - Mechanisms and Models (H. Bockhorn, Ed.)*, Springer Verlag, p. 165.

[13] Garo, A., Said, R. and R., B. (1994). *Soot Formation in Combustion - Mechanisms and Models (H. Bockhorn, Ed.)*, Springer Verlag, p. 527.

[14] Haynes, B. and Wagner, H. (1981). *Prog. Energy Combust. Sci.* **7**: 229.

[15] Huth, M. and Leuckel, W. (1994). *Soot Formation in Combustion -Mechanisms and Models (H. Bockhorn, Ed.),*, Springer Verlag, p. 371.

[16] Janicka, J., Kolbe, W. and Kollmann, W. (1979). *J. Non-Equilib. Thermodyn.* **4**: 47.

[17] Kazakov, A. and Frenklach, M. (1998). *Combust. Flame* **114**: 484.

[18] Kazakov, A., Wang, H. and Frenklach, F. (1995). *Combust. Flame* **100**: 111.

[19] Kennedy, I. M. (1997). *Prog. Energy Combust. Sci.* **23**: 95.

[20] Kollmann, W., Kennedy, I. M., Metternich, M. and Chen, J.-Y. (1994). *Soot Formation in Combustion -Mechanisms and Models (H. Bockhorn, Ed.)*, Springer Verlag, p. 503.

[21] Kraft, M. (1998). *Stochastic Modelling of Turbulent Reacting Flow in Chemical Engineering*, number 391 in *Fortschrittsberichte des VDI, Reihe 6*, Dusseldörf: VDI Verlag.

[22] Kraft, M., Balthasar, M. and Mauss, F. (1999). *Scientific computing in chemical engineering (Vol. 2) (F. Keil, Ed.)*, Springer-Verlag, Berlin, p. 118.

[23] Libby, P. A. and Williams, F. (1993). *Turbulent Reactive Flow*, Springer Verlag, New York.

[24] Lockwood, F. C. and van Niekerk, J. E. (1995). *Combust. Flame* **103**: 76.

[25] Mauss, F. (1998). *PhD thesis: Entwicklung eines kinetischen Modells der Russbildung mit schneller Polymerisation*, RWTH Aachen, Department of Mechanical Engineering.

[26] Mauss, F. and Bockhorn, H. (1995). *Phys. Chem.* **188**: 45.

[27] Mauss, F., Schäfer, T. and Bockhorn, H. (1994a). *Combust. Flame* **99**: 697.

[28] Mauss, F., Trilken, B., Breitbach, H. and Peters, N. (1994b). *Soot Formation in Combustion -Mechanisms and Models (H. Bockhorn, Ed.)*, Springer Verlag, p. 325.

[29] Pitsch, H., Barths, H. and Peters, N. (1996). *SAE 962057*.

[30] Pope, S. B. (1982). *Combust. Sci. and Tech.* **28**: 131.

[31] Pope, S. B. (1985). *Prog. Energy Combust. Sci.* **11**: 119.

[32] Pope, S. B. (1995). *J. Comput. Phys.* **117**: 332.

[33] Procaccini, C., Kraft, M., Fey, H., Bockhorn, H., Longwell, J. P., Sarofim, A. and Smith, K. A. (1998). *Proc. Combust. Inst.* **27**: 1275.

[34] Saffman, P. G. and Turner, J. S. (1956). *Fluid Mech.* **1**: 16.

[35] Seinfeld, J. H. (1986). *Atmospheric Chemistry and Physics of Air Pollution*, John Wiley & Sons, New York, USA, p. 397.

[36] Steward, C. D., Syed, K. J. and Moss, J. B. (1990). *Combust. Sci. and Tech.* **75**: 211.

[37] Valiño, L. and Dopazo, C. (1991). *Phys. Fluids.* **3**(12): 3034.

[38] Vohler, O., von Sturm, F., Wege, E., von Kienle, H., Voll, M. and Kleinschmitt, P. (1986). *Ullmanns Encyclopedia of Industrial Chemistry*, VCH, Weinheim, pp. 95–163.

[39] Von Smoluchowski, M., Z. (1917). *Phys. Chem.* **92**: 129.

[40] Williams, M. M. R. and Loyalka, S. K. (1991). *Aerosol Science Theory and Practice*, Pergamon Press, Oxford.

[41] Yoshihara, Y., Kazakov, A., Wang, H. and Frenklach, M. (1998). *Proc. Combust. Inst.* **25**: 941.

A Appendices

A.1 Consistency of IEM mixing model

We start from the basic equation of the IEM-model for soot particles of size i,

$$\frac{dN_i^{(n)}}{dt} = \frac{C_\phi}{2\tau}\left(N_i^{(n)} - \langle N_i \rangle\right) = \frac{C_\phi}{2\tau}\left(N_i^{(n)} - \left(\frac{1}{N}\sum_{n=1}^{N} N_i^{(n)}\right)\right), \quad i = 1, \ldots, \infty, \tag{A.1}$$

where $N_i^{(n)}$ is the number density of particles of size i of the stochastic particle n and N the total number of stochastic particles.

The sum over all size classes multiplied with the $r-$th power of i can be formed:

$$\frac{d\left(\sum_{i=1}^{\infty} i^r N_i^{(n)}\right)}{dt} = \sum_{i=1}^{\infty} i^r \frac{C_\phi}{2\tau}\left[N_i^{(n)} - \left(\frac{1}{N}\sum_{n=1}^{N} N_i^{(n)}\right)\right]. \tag{A.2}$$

Using the definition of the moments (Eq.2) we obtain an equation, which determines how the moments of the PSDF have to be mixed

$$\frac{dM_r^{(n)}}{dt} = \frac{C_\phi}{2\tau}\left[M_r^{(n)} - \frac{1}{N}\sum_{n=1}^{N} M_r^{(n)}\right]. \tag{A.3}$$

This equation is identical to $dM_r^{(n)}/dt = C_\phi/(2\tau)(M_r^{(n)} - \langle M_r \rangle)$ and consequently we conclude that the IEM model fulfils the consistency requirements.

A.2 Consistency of Curl's Mixing Model

The proof for Curl's mixing model is performed in the same manner as that for the IEM model. We start from the basic equation for the number density of soot particles having size i

$$N_i^{(n)}(t + \Delta t) = N_i^{(m)}(t + \Delta t) = \frac{1}{2}\left(N_i^{(n)}(t) + N_i^{(m)}(t)\right), \quad i = 1, \ldots, \infty. \tag{A.4}$$

Multiplying by i^r and summing over all size classes from $i=1,\ldots,\infty$, we obtain

$$\sum_{i=1}^{\infty} i^r N_i^{(n)}(t + \Delta t) = \sum_{i=1}^{\infty} i^r N_i^{(m)}(t + \Delta t) = \frac{1}{2}\left(\sum_{i=1}^{\infty} i^r N_i^{(n)}(t) + \sum_{i=1}^{\infty} i^r N_i^{(m)}(t)\right). \tag{A.5}$$

Using the definition of the moments M_r, the mixing model in moment form is as follows:

$$M_r^{(n)}(t + \Delta t) = M_r^{(m)}(t + \Delta t) = \frac{1}{2}\left(M_r^{(n)}(t) + M_r^{(m)}(t)\right), \tag{A.6}$$

which proves consistency. This proof applies to the modified Curl model as well.

A.3 Consistency of the Binomial Langevin model

The Binomial Langevin model applied to the number densities of soot particles writes as:

$$\begin{aligned} dN_i^{(n)} = &-\frac{C_\phi}{2\tau}\left(1 + k_{BL}(1 - \frac{\langle N'^2_i\rangle}{\psi_*^2})\right)(N_i^{(n)} - \langle N_i\rangle)dt \\ &+ \left(k_{BL}\frac{C_\phi}{2\tau}\left(1 - \frac{(N_i^{(n)} - \langle N_i\rangle)^2}{\psi_*^2}\right)\langle N_i^2\rangle\right)^{\frac{1}{2}} dW_{bl}. \end{aligned} \tag{A.7}$$

We start by considering part of the expression only, i.e. the first term on the right hand side of equation Eq.(A.7):

$$T_1 = -\frac{C_\phi}{2\tau}(N_i^{(n)} - \langle N_i\rangle) - \frac{C_\phi}{2\tau}k_{BL}(N_i^{(n)} - \langle N_i\rangle) + \frac{C_\phi}{2\tau}k_{BL}\frac{\langle N'^2_i\rangle}{\psi_*^2}(N_i^{(n)} - \langle N_i\rangle). \tag{A.8}$$

The first two terms of Eq.(A.8) have the same form as the equation for the IEM mixing model Eq.(A.1) and are consequently transformed into the moment form as shown in section A.1. We will therefore only focus on the third term in Eq.(A.8) which is more complex. Starting by multiplying Eq.(A.8) with i^r and summing Eq.(A.8) over all size classes $i$we get for the special case of $\langle N_i\rangle = 0$:

$$\sum_{i=1}^{\infty} i^r k_{BL}\frac{C_\phi}{2\tau}\left(\frac{1}{N}\sum_{n=1}^{N} N_i^{(n)2}\right)\frac{N_i^{(n)}}{\psi_*^2} \neq k_{BL}\frac{C_\phi}{2\tau}\langle M_r^2\rangle\frac{M_r^{(n)}}{\psi_*^2} \tag{A.9}$$

As the number density appears in a non-linear form in the term of the left hand side of Eq.(A.9) we find that the expression for particle sizes is not consistent with mixing the moments of the PSDF. Failure of closure of Eq.(A.9) implies failure of the Binomial Langevin mixing model if independence of the different terms in Eq.(A.7) is assumed.